Biochemistry
Article
Cite This: Biochemistry XXXX, XXX, XXX−XXX
pubs.acs.org/biochemistry

Peroxidase versus Peroxygenase Activity: Substrate Substituent Effects as Modulators of Enzyme Function in the Multifunctional Catalytic Globin Dehaloperoxidase

Ashlyn H. McGuire, Leiah M. Carey, Vesna de Serrano, Safaa Dali, and Reza A. Ghiladi*

Department of Chemistry, North Carolina State University, Raleigh, North Carolina 27695-8204, United States

Supporting Information

ABSTRACT: The dehaloperoxidase-hemoglobin (DHP) from the terebellid polychaete *Amphitrite ornata* is a multifunctional hemoprotein that catalyzes the oxidation of a wide variety of substrates, including halo/nitrophenols, haloindoles, and pyrroles, via peroxidase and/or peroxygenase mechanisms. To probe whether substrate substituent effects can modulate enzyme activity in DHP, we investigated its reactiviy against a panel of *o*-guaiacol substrates given their presence (from native/halogenated and non-native/anthropogenic sources) in the benthic environment that *A. ornata* inhabits. Using biochemical assays supported by spectroscopic, spectrometric, and structural studies, DHP was found to catalyze the H_2O_2-dependent oxidative dehalogenation of 4-haloguaiacols (F, Cl, and Br) to 2-methoxybenzoquinone (2-MeOBQ). ^{18}O labeling studies confirmed that O atom incorporation was derived exclusively from water, consistent with substrate oxidation via a peroxidase-based mechanism. The 2-MeOBQ product further reduced DHP to its oxyferrous state, providing a link between the substrate oxidation and O_2 carrier functions of DHP. Nonnative substrates resulted in polymerization of the initial substrate with varying degrees of oxidation, with 2-MeOBQ identified as a minor product. When viewed alongside the reactivity of previously studied phenolic substrates, the results presented here show that simple substituent effects can serve as functional switches between peroxidase and peroxygenase activities in this multifunctional catalytic globin. More broadly, when recent findings on DHP activity with nitrophenols and azoles are included, the results presented here further demonstrate the breadth of heterocyclic compounds of anthropogenic origin that can potentially disrupt marine hemoglobins or function as environmental stressors, findings that may be important when assessing the environmental impact of these pollutants (and their metabolites) on aquatic systems.

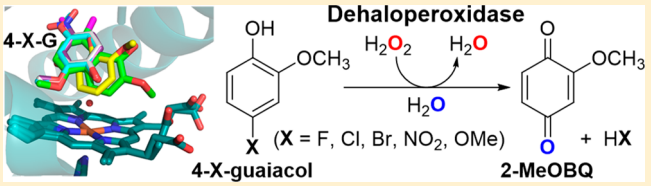

Downloaded via NORTH CAROLINA STATE UNIV on July 25, 2018 at 19:29:35 (UTC).
See https://pubs.acs.org/sharingguidelines for options on how to legitimately share published articles.

Guaiacol (methoxyphenol), a major component of wood lignin, is released into the environment from both anthropogenic and natural sources,[1−3] some examples of which include (i) biomass burning, where during the combustion of wood lignin the semivolatile guaiacol-derived pollutants can be aerosolized, enter the troposphere, and can further react with atmospheric nitrogen-containing species to yield nitroguaiacols,[4] which are generally considered to be more toxic than the parent compound, (ii) the paper-pulp industry, where during the bleaching of wood pulp the bleaching agents (molecular chlorine, hypochlorite, etc.) react with lignin, resulting in chlorinated phenolic derivatives (i.e., chloroguaiacols and chlorocatechols), and (iii) derivatives of polybrominated diphenyl ethers that originate both artificially (from chemical transformations of polybrominated flame-retardant chemicals) and naturally (as biosynthetic compounds produced by marine bacteria).[5] These compounds are then released into the environment through wastewater effluent[2,6] or via precipitation,[7,8] leading to contamination of both water and soil. With recent reports demonstrating that guaiacol pollutants are acutely toxic to a level that meets the European toxicity classification of "harmful",[9] there is an increasing need to assess the impact of these compounds, including their metabolites, on the environment.

Although enzyme-catalyzed guaiacol oxidation has been extensively examined,[10−16] most studies have focused on enzymes from microbial or plant origins. As such, the mechanisms by which infaunal organisms cope with guaiacol pollutants as environmental stressors, produced either natively as halometabolites by other organisms or from anthropogenic sources, remain relatively understudied by comparison. Our platform for exploring the interactions of such environmental pollutants with infaunal organisms is *Amphitrite ornata*, a sediment-dwelling marine polychaete.[17] Inhabiting coastal mudflats that are rich in biogenically produced halometabolites excreted from other organisms,[18] *A. ornata* faces stressors that include brominated indoles, pyrroles, phenols, and—of particular relevance to this study—guaiacols. To overcome the challenges posed by this diverse array of toxic haloaromatic compounds, *A. ornata* employs its hemoglobin to function both as a detoxification enzyme and as an O_2-transport protein.[19−21] Named dehaloperoxidase (DHP), this coelomic hemoglobin[22] possesses an unusually broad substrate profile encompassing halophenols,[20,23] haloindoles,[24] and (halo)-

Received: May 11, 2018
Revised: June 19, 2018
Published: June 27, 2018

ACS Publications © XXXX American Chemical Society

DOI: 10.1021/acs.biochem.8b00540
Biochemistry XXXX, XXX, XXX−XXX

pyrroles[25] and as such is the first known multifunctional catalytic globin to possess biologically relevant peroxidase[26−33] and peroxygenase[24,25,34] activities, as well as an oxidase[24] activity that leads to the formation of indigo derivatives. DHP also exhibits activity against compounds of anthropogenic origin, including the H_2O_2-dependent oxidation of mono- and dinitrophenols,[34] and is also capable of binding azole species,[35] including imidazole, benzotriazole, benzimidazole, and indazole.

DHP has two isoenzymes encoded by separate genes,[36] A and B, which differ by only five amino acid substitutions (isoenzyme A is listed first): I/L9, R/K32, Y/N34, N/S81, and S/G91. Although these two isoenzymes are structurally identical,[37] DHP B consistently exhibits a reactivity greater than that of isoenzyme A, and as such, recent studies have focused on this variant.[29] Mechanistic studies have shown that both isoenzymes appear to function via a Poulos−Kraut type mechanism:[38] ferric DHP reacts with H_2O_2 to form DHP Compound I,[39] an iron(IV)−oxo porphyrin π-cation radical species. In wild type (WT) DHP, Compound I rapidly converts in DHP to an iron(IV)−oxo heme center with a tyrosyl radical that has been termed Compound ES[32,33,40] by analogy with cytochrome *c* peroxidase, whereas in mutants such as DHP B (Y28F/Y38F),[31] the Compound I species can be investigated directly. These peroxide-activated forms of DHP initially return to the ferric resting state upon substrate oxidation, although further reduction to oxyferrous DHP has been noted under some conditions.[24,25,34,40,41]

Given the diverse functions (O_2 carrier, peroxidase, peroxygenase, and oxidase) exhibited by DHP across this broad panel of substrates, we have previously suggested that the substrate itself can act to modulate enzyme activity in DHP,[29,30] with binding/orientation (relative to the ferryl iron), pK_a, and redox potential all being key determinants in terms of which mechanism leads to substrate oxidation. More interestingly, however, it also appears that substituent effects may play a pseudoallosteric role (Figure 1): the peroxidase substrate phenol is converted to a peroxygenase substrate upon addition of a 4-nitro substituent,[34] whereas 4-Br-phenol is an inhibitor[42] of peroxidase and peroxygenase activities in DHP. These substituent effects suggest that it may be possible to modulate DHP activity by switching the substrate oxidation mechanism, not through traditional mutagenesis or heme cofactor modification but through selection of the substrate itself.

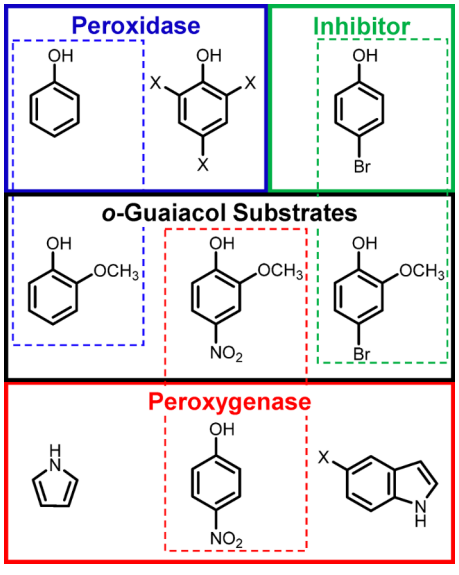

Figure 1. DHP peroxidase (blue), peroxygenase (red), and oxidase (green) substrates and *o*-guaiacol structures (black) (X = F, Cl, Br, or I).

To investigate how guaiacol pollutants may undergo biotransformations by infaunal organisms and to probe the role of substituent effects as modulators and/or regulators of the multiple activities in DHP, we evaluated a panel of 4-X-guaiacol (X = F, Cl, Br, NO_2, OMe, or Me) substrates using a combination of spectroscopic methods, biochemical assays, and isotope labeling studies. The basis for selecting guaiacols (Figure 1) within the context of substituent/electronic effects is as follows. (i) The addition of the methoxy substituent to phenol (blue box), 4-nitrophenol (red box), and 4-Br-phenol (green box) will enable us to probe its effect on the peroxidase,[19] peroxygenase,[24,25,34] and inhibition[42] pathways of DHP relevant to the putative guaiacol substrates. (ii) Haloguaiacols are native to the benthic environment of *A. ornata*[18,43] and likely represent physiologically relevant substrates, while anthropogenic analogues, such as 4-nitroguaiacol[4] and 4-chloroguaiacol,[2] are relevant as environmental stressors. (iii) Guaiacol oxidation is well understood with respect to monofunctional heme proteins[10,13,14,44] but is unknown with respect to multifunctional catalytic globins. As will be shown, the results establish that guaiacols are indeed substrates for DHP and demonstrate that simple substituent effects can be used as a functional switch between peroxidase and peroxygenase activities in modulating the activity of this multifunctional catalytic globin. More broadly, when viewed along with our recent findings employing nitrophenols[34] and azoles,[35] the results further demonstrate the breadth of heterocyclic compounds of anthropogenic origin that can potentially disrupt marine hemoglobins or function as environmental stressors, findings that may be important when assessing the environmental impact of these pollutants (and their metabolites) on aquatic systems.

EXPERIMENTAL PROCEDURES

Materials. Ferric samples of WT DHP B were expressed and purified as previously reported.[37,40] Oxyferrous DHP B was prepared by the aerobic addition of excess ascorbic acid to ferric DHP B, followed by removal of the reducing agent via a PD-10 desalting column.[41] The enzyme concentration was determined spectrophotometrically using an ε_{Soret} of 116400 M^{-1} cm^{-1}.[40] Horse skeletal muscle (HSM) myoglobin and horseradish peroxidase (HRP) were purchased from Sigma-Aldrich, and enzyme concentrations were determined using ε_{Soret} values of 188000 M^{-1} cm^{-1}[45] and 102000 M^{-1} cm^{-1},[46] respectively. Solutions of H_2O_2 were prepared fresh daily in 100 mM KP_i (pH 7) and kept on ice until they were needed. Isotopically labeled $H_2{}^{18}O_2$ (90% ^{18}O-enriched) and $H_2{}^{18}O$ (98% ^{18}O-enriched) were purchased from Icon Isotopes (Summit, NJ). Stock solutions of guaiacols (10 mM) were prepared in MeOH and stored in the dark at −80 °C until they were needed. Acetonitrile (MeCN) was high-performance liquid chromatography (HPLC) grade, and all other reagent grade chemicals were purchased from VWR, Sigma-Aldrich, or Fisher Scientific and used without further purification.

Guaiacol Binding Studies. The guaiacol substrate dissociation constants (K_d) were determined in triplicate for

DOI: 10.1021/acs.biochem.8b00540
Biochemistry XXXX, XXX, XXX−XXX

DHP in 100 mM KP_i (pH 7) containing 6.25% MeOH at 25 °C using a Cary 50 ultraviolet−visible (UV−vis) spectrophotometer per previously published protocols.[24,47] The UV−vis spectrometer was referenced with 50 μM WT DHP B in 100 mM KP_i (pH 7) in 6.25% MeOH. Spectra were acquired in the presence of guaiacol substrate concentrations (3.75−50 equiv) while constant DHP B (50 μM) and methanol concentrations were maintained. Analyses of the Q-band region (450−600 nm) were performed using the ligand binding function in Grafit (Erithacus Software Ltd.).

HPLC Activity Studies. Reactions were performed in triplicate at pH 7 (unless otherwise indicated) in 100 mM KP_i containing 5% MeOH at 25 °C. Assay components (250 μL final volume) included 10 μM enzyme and 500 μM substrate (in MeOH), and the reaction was initiated by the addition of 500 μM H_2O_2. Experiments were also performed in the presence of 500 μM 4-bromophenol, 500 μM D-mannitol, 100 mM 5,5-dimethyl-1-pyrroline *N*-oxide (DMPO, in MeOH), or 10% (v/v) dimethyl sulfoxide (DMSO), which was added prior to the addition of H_2O_2. The reactions were quenched after 5 min with excess catalase. A 100 μL aliquot was diluted 10-fold with 900 μL of 100 mM KP_i (pH 7). The samples were analyzed using a Waters 2796 Module coupled with a Waters 2996 photodiode array detector and equipped with a Thermo Fisher Scientific ODS Hypersil (150 mm × 4.6 mm) 5 μm particle size C_{18} column. Separation was performed using a linear gradient of binary solvents (solvent A, H_2O and 0.1% TFA; solvent B, acetonitrile and 0.1% TFA). The elution consisted of the following conditions: (1.5 mL/min A:B) 95:5 to 5:95 linearly over 12 min, 5:95 isocratic for 2 min, 5:95 to 95:5 over 1 min, and then isocratic for 3 min. Data analysis was performed using the Waters Empower software package.

Product Determination by Liquid Chromatography−Mass Spectrometry (LC−MS). Analysis was performed on a Thermo Fisher Scientific Exactive Plus Orbitrap mass spectrometer using a heated electrospray ionization (HESI) probe. The samples were introduced via LC injection into the mass spectrometer at a flow rate of 250 μL/min (solvent A, H_2O and 0.1% formic acid; solvent B, acetonitrile and 0.1% formic acid) after elution from a Thermo Hypersil Gold (50 mm × 2.1 mm, 1.9 μm particle size) C_4 column. The mass spectrometer was operated in positive and negative modes. Spectra were collected while scanning from m/z 100 to 1500. Data analysis was performed using Thermo Xcalibur software. The assay included 10 μM DHP B, 500 μM substrate, and 500 μM H_2O_2 in buffer [5 mM KP_i (pH 7)] with a final volume of 250 μL and was allowed to react for 5 min before being quenched with catalase. A 20 μL aliquot of the undiluted reaction mixture was injected for LC−MS analysis. For the ^{18}O labeling studies, unlabeled H_2O_2 was replaced with $H_2{}^{18}O_2$, and/or the KP_i buffer was replaced with $H_2{}^{18}O$ to ensure >90% labeled $H_2{}^{18}O$.

Stopped-Flow UV−Vis Spectroscopy Studies. Optical spectra were recorded using a Bio-Logic SFM-400 triple-mixing stopped-flow instrument coupled to a rapid scanning diode array UV−vis spectrophotometer. Protein and hydrogen peroxide solutions were prepared in 100 mM KP_i (pH 7), and the guaiacol substrates were dissolved in buffer containing 4% methanol. Data were collected (900 scans total) over a three-time domain (1.5, 15, and 150 ms) using the Bio-Kine 32 software package (Bio-Logic). All data were evaluated using the Specfit Global Analysis System software package (Spectrum Software Associates) and fit with SVD analysis as either one-step, two-species or two-step, three-species irreversible mechanisms, where applicable. For data that did not properly fit these models, experimentally obtained spectra at selected time points detailed in the figure legends are shown. Kinetic data were baseline-corrected using the Specfit autozero function when appropriate.

Double-mixing experiments were performed using an aging line prior to the second mixing step to observe Compound I/ES/II reactivity with the guaiacol substrates (5−50 equiv). (i) Compound I was preformed by the reaction of ferric DHP B (Y28F/Y38F) with 10 equiv of H_2O_2 in an aging line for 85 ms[31] prior to mixing with the substrate. (ii) Compound ES was preformed by reaction of ferric WT DHP B with 10 equiv of H_2O_2 in an aging line for 500 ms.[40] (iii) Compound II was formed from oxyferrous DHP B preincubated with 1 equiv of TCP and reacted with 10 equiv of H_2O_2 in an aging line for 3 s.[41]

Protein Crystallization and X-ray Diffraction Studies. Non-His-tagged DHP B was overexpressed and purified as described in the literature.[29,30,37] DHP B crystals were obtained using the hanging-drop vapor diffusion method. The crystals were grown from mother liquor solutions of 32% PEG 3350 and 0.2 M ammonium sulfate at pH 6.4 and equilibrated against identical reservoir solutions. Protein:-mother liquor ratios varied (1:1, 1.33:1, 1.66:1, and 2:1). At 4 °C, crystals grew from each condition after 3 days. The crystals were soaked for 12 h in substrate-enhanced reservoir solutions identical to the mother liquor. Substrate final concentrations were all 100 mM [5% (v/v) DMSO]. The crystals were cryoprotected by being briefly dipped in a reservoir solution containing 20% glycerol and then cryocooled in liquid N_2. Data were collected at 100 K on the SER-CAT 22-BM beamline at the APS synchrotron facility, utilizing a wavelength of 1.00 Å. All data were scaled and integrated using HKL2000,[48] and molecular replacement was performed with Phaser-MR[49] from the PHENIX[50] and CCP4[51] suite of programs using 3IXF[37] as the search model. Model building and manual placement of waters utilized COOT,[52] and refinement was performed using refmac[53] and phenix.refine.[54]

RESULTS

DHP-Catalyzed Guaiacol Reactivity with H_2O_2. The hydrogen peroxide-dependent reaction of ferric DHP B with guaiacol substrates at pH 7 was monitored via HPLC, and the corresponding substrate conversion percentages are listed in Table 1. Reactions were initiated upon addition of 500 μM H_2O_2 to a solution containing 10 μM enzyme and 500 μM guaiacol, mixtures incubated at 25 °C for 5 min, and then reactions quenched with catalase. With the exception of *o*-guaiacol (67.6%), all substrates exhibited very high conversion, with the 4-X-guaiacol series (X = F, Cl, or Br) essentially being fully oxidized (>99.7%) and 5- and 6-Br-guaiacol only slightly diminished. Non-native guaiacol substrates (4-NO_2-, 4-Me-, and 4-MeO-guaiacol) were also found to be very reactive (92.8−98.6%). No turnover of substrate was observed in the absence of H_2O_2 (non-oxidant control) or enzyme (non-enzymatic control).

Using 4-Br-guaiacol as a representative substrate because of its similarity to previously studied halophenols,[55] the following observations were noted. (i) A minimal pH effect was observed (pH 5 < pH 7 ≈ pH 8). (ii) Substrate conversions were also found to be identical when the assays were initiated from the oxyferrous ("hemoglobin-like") or ferric ("peroxidase-like")

DOI: 10.1021/acs.biochem.8b00540
Biochemistry XXXX, XXX, XXX−XXX

Table 1. DHP-Catalyzed Oxidation of Substituted Guaiacols[a]

substrate	conversion (%)
Substrate Variation	
ferric WT DHP B, pH 7	
with *o*-guaiacol	67.6 ± 0.2
with 4-F-guaiacol	>99.9
with 4-Cl-guaiacol	99.7 ± 0.1
with 4-Br-guaiacol	99.7 ± 0.2
with 5-Br-guaiacol	90.0 ± 1.0
with 6-Br-guaiacol	88.8 ± 0.2
with 4-NO_2-guaiacol	92.8 ± 0.2
with 4-MeO-guaiacol	94.6 ± 1.2
with 4-Me-guaiacol	98.6 ± 0.3
pH Studies (4-Br-guaiacol)	
pH 5	90.5 ± 0.2
pH 8	99.6 ± 0.1
Enzyme Variation	
oxyferrous WT DHP B	
with 4-Br-guaiacol	99.7 ± 0.1
with 5-Br-guaiacol	84.8 ± 2.0
HRP	
with 4-Br-guaiacol, pH 6	>99.9
myoglobin (HSM)	
with 4-Br-guaiacol	29.3 ± 2.8
with 5-Br-guaiacol	32.9 ± 2.0
Mechanistic Probes (ferric WT DHP B)	
4-Br-guaiacol	
with 500 μM mannitol	99.7 ± 0.2
with 10% DMSO	99.6 ± 0.1
with 100 mM DMPO	99.4 ± 0.2
with 500 μM 4-bromophenol	84.8 ± 0.1
anaerobic	99.7 ± 0.2
without H_2O_2	no reactivity detected
without enzyme	no reactivity detected
5-Br-guaiacol	
with 100 mM DMPO	27.6 ± 1.1
4-NO_2-guaiacol	
with 100 mM DMPO	28.5 ± 1.3

[a]Reaction conditions: 10 μM enzyme, 500 μM guaiacol, 500 μM H_2O_2, 5% MeOH/100 mM KP_i (v/v), pH 7 unless otherwise noted.

oxidation states, in line with previous observations for DHP for the oxidation of TCP via a peroxidase mechanism,[41] and the oxidation of haloindoles,[24] nitrophenols,[34] and pyrroles[25] via a peroxygenase cycle. (iii) Both DHP B and the canonical peroxidase HRP yielded complete conversion of the substrate to product(s), although the product distributions were found to be different (*vide infra*). (iv) Horse skeletal muscle myoglobin exhibited a 3.4-fold attenuation of reactivity. These results support that DHP reactivity with guaiacols is on a par with those of classical peroxidase enzymes yet is greater than those of other members of the globin family.

Mechanistic studies were also employed to elucidate key details of the reaction of 4-Br-guaiacol with DHP. Under anaerobic conditions, substrate conversion (99.7%) was identical to the aerobic reaction, showing no dependence on molecular oxygen. The addition of the hydroxyl radical scavengers D-mannitol (99.7%) and dimethyl sulfoxide (DMSO; 99.6%) also had no effect on the oxidation of 4-Br-guaiacol, suggesting that freely diffusible hydroxyl radicals are not involved in the reaction. Similarly, the radical scavenger 5,5-dimethyl-1-pyrroline *N*-oxide (DMPO) did not show reduced 4-Br-guaiacol reactivity (99.4%). However, DMPO did significantly inhibit substrate conversion of 5-Br-guaiacol (27.6 ± 1.1% vs 90.0 ± 1.0%) and 4-NO_2-guaiacol (28.5 ± 1.3% vs 92.8 ± 0.2%), indicating a difference between these substrates pertaining to the diffusibility of substrate radicals (*vide infra*). When the peroxidase and peroxygenase inhibitor 4-bromophenol (K_d = 1.15 mM[42,56]) was added, substrate conversion was minimally decreased by 1.2-fold, suggesting that 4-bromophenol has an only slight inhibitory effect on 4-Br-guaiacol oxidation.

Identification of Reaction Products by HPLC and LC–MS. The HPLC chromatograms for the reaction of ferric WT DHP B with guaiacol substrates are shown in Figure 2 and

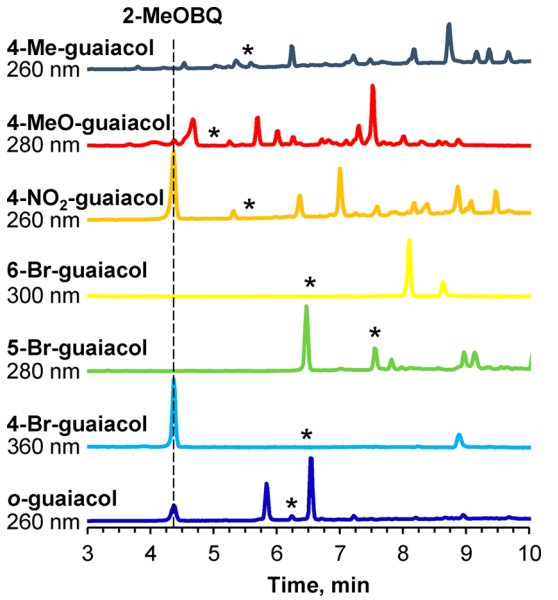

Figure 2. HPLC chromatograms at the indicated detection wavelength depicting the reaction of DHP B with guaiacol substrates. Reaction conditions: 10 μM DHP B, 500 μM guaiacol, 500 μM H_2O_2, 5% MeOH/100 mM KP_i (v/v) at pH 7. The reaction was quenched after 5 min with the addition of excess catalase (t_R = 9 min). The 2-MeOBQ product is highlighted at a t_R of 4.5 min. Asterisks denote retention times of the initial substrate.

Figure S1, and lists of the products by their retention times and masses are provided in Tables S1 and S2. Although identification of the exact chemical structures was not pursued, the products generally consisted of dimers, trimers, and tetramers with varying degrees of oxidation, in line with previous reports for heme enzyme-catalyzed oxidation of guaiacol.[10,57−59] For the 4-X-guaiacols (X = F, Cl, or Br), dehalogenation products were also identified, an expected result given the DHP-catalyzed oxidative dehalogenation of 2,4,6-trihalophenols to their corresponding 2,6-dihaloquinones has been well-established.[19,55]

Interestingly, a common product with a characteristic retention time (t_R) of 4.5 min was observed in the oxidation of six substrates: *o*-guaiacol, 4-X-guaiacol (X = F, Cl, or Br), 4-MeO-guaiacol, and 4-NO_2-guaiacol. This product exhibited a retention time, a UV–vis spectrum (Figure S2), and a mass (m/z 139.04, $[M + H]^+$) identical to those of an authentic commercial sample of 2-methoxy-1,4-benzoquinone (2-MeOBQ; see Figure S3 for the corresponding calibration

DOI: 10.1021/acs.biochem.8b00540
Biochemistry XXXX, XXX, XXX−XXX

curve). The amount of 2-MeOBQ produced varied 10-fold across these six substrates: 4-F-guaiacol (398 ± 14 μM), 4-Cl-guaiacol (397 ± 23 μM), 4-Br-guaiacol (374 ± 3 μM), 4-MeO-guaiacol (231 ± 1 μM), 4-NO_2-guaiacol (42 ± 3 μM), and *o*-guaiacol (35 ± 1 μM), representing 80, 79, 75, 46, 8.3, and 7.0% of the starting material being converted to 2-MeOBQ, respectively. Formation of 2-MeOBQ implies dehalogenation (-HX, X = F^-, Cl^-, or Br^-), loss of methanol (-MeOH), or loss of nitrite (HNO_2) from the aforementioned substrates, although no attempts to identify the leaving groups were made. No such 2-MeOBQ product was seen in the reactions with 4-Me-guaiacol, 5-Br-guaiacol, or 6-Br-guaiacol. In the presence of the radical scavenger DMPO, the 2-MeOBQ product was unaffected for the 4-Br-guaiacol reaction; however, no 2-MeOBQ was observed when DMPO was included in the reaction with 4-NO_2-guaiacol, and fewer product peaks were noted in the reaction with 5-Br-guaiacol (data not shown).

Isotopically Labeled Oxygen Studies. To determine the origin of the O atom incorporated into the 2-MeOBQ product, studies employing labeled $H_2{}^{18}O$ and $H_2{}^{18}O_2$ (98% and 90% ^{18}O-enriched, respectively) were performed with 4-Br-guaiacol as the substrate, and the results were subsequently analyzed by LC−MS. The corresponding background-subtracted total ion chromatograms (TICs) are shown in Figure 3. In the presence of unlabeled H_2O and $H_2{}^{18}O_2$, no significant increase in mass was observed [*m*/*z* 139.04 (Figure 3A)], when compared to that under the unlabeled H_2O/H_2O_2 conditions [*m*/*z* 139.04 (data not shown)], suggesting that the source of O atom incorporation was not H_2O_2. The reaction employing $H_2{}^{18}O$ and unlabeled H_2O_2 resulted in increases of 2 and 4 Da in 2-MeOBQ [*m*/*z* 139.04, 4.9%; *m*/*z* 141.04, 38.1%; *m*/*z* 143.04, 57.0% (Figure 3B)], suggesting scrambling from solvent was occurring for both O atoms in 2-MeOBQ. Importantly, the $H_2{}^{18}O/H_2{}^{18}O_2$ double-label reaction produced results [*m*/*z*, 139.04, 6.1%; *m*/*z* 141.04, 40.3%; *m*/*z* 143.04, 53.6% (Figure 3C)] similar to those of the $H_2{}^{18}O/H_2{}^{16}O_2$ reaction, providing unequivocal evidence that the O atom was derived exclusively from H_2O with no O atom incorporation from H_2O_2, consistent with a peroxidase mechanism for guaiacol oxidation by DHP.

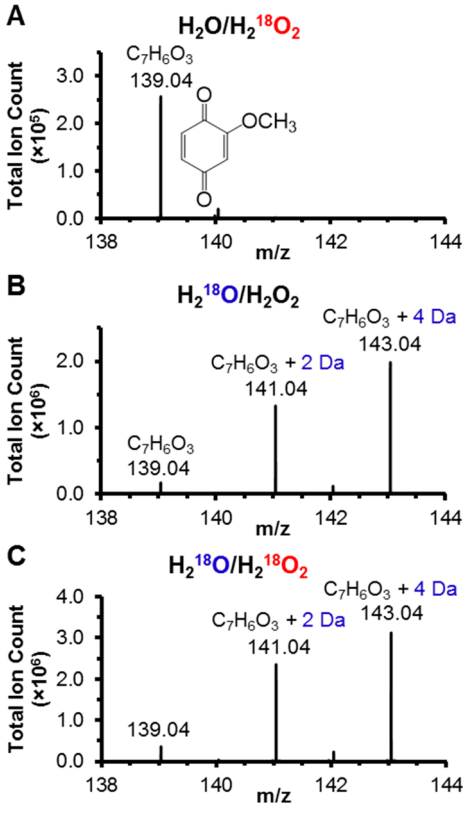

Figure 3. ESI-MS total ion chromatogram for the DHP B and 4-Br-guaiacol reaction product: (A) $H_2{}^{16}O/H_2{}^{18}O_2$, (B) $H_2{}^{18}O/H_2{}^{16}O_2$, and (C) $H_2{}^{18}O/H_2{}^{18}O_2$. Reaction conditions: 10 μM DHP, 500 μM 4-Br-guaiacol, 500 μM H_2O_2, 5% MeOH/100 mM KP_i (v/v), pH 7, 25 °C.

Guaiacol Binding Studies. The electronic absorption spectra of ferric DHP B in the presence of guaiacol substrates were recorded in 100 mM KP_i (pH 7) containing 6.25% (v/v) MeOH. No significant systematic changes in the Soret band were observed upon ligand binding (data not shown), thus precluding its use for substrate binding studies. The Q-band region, however, showed well-behaved optical difference spectra (Figures S4 and S5) upon titration of the guaiacol substrates (3.75−100 equiv), enabling the determination of the corresponding apparent dissociation constants (K_d values). In general, the substituted guaiacols exhibited weaker binding affinities for ferric DHP B than for other substrates/ligands, including haloindoles,[24] nitrophenols,[34] and azoles[35] (Table 2). For the 4-X-guaiacol panel of substrates, a trend in K_d was observed of increasing binding affinity as the size of the halogen atom increased: H < F < Cl < Br. An identical trend has been previously noted for the 5-X-indole series (F < Cl < Br < I) as observed in both substrate binding and resonance Raman studies[24] and correlates well with the increased affinity of the halogen for occupying the Xe1 binding site (a

Table 2. K_d Values for Substrate Binding to Ferric WT DHP B at pH 7

substrate	K_d (μM) at pH 7	ref
guaiacol		
o-guaiacol	14712 ± 714	*a*
4-F-G	2438 ± 207	*a*
4-Cl-G	493 ± 53	*a*
4-Br-G	374 ± 42	*a*
4-MeO-G	*b*	*a*
4-Me-G	1433 ± 97	*a*
4-NO_2-G	1341 ± 26	*a*
5-Br-G	1745 ± 340	*a*
6-Br-G	1332 ± 342	*a*
phenol		
4-BP	1150	56
4-NP	262 ± 23	34
2,4-DNP	105 ± 21	34
indole		
5-Cl-indole	317 ± 23	24
5-Br-indole	150 ± 10	24
5-I-indole	62 ± 10	24
azole		
imidazole	52 ± 2	35
benzotriazole	82 ± 2	35
benzimidazole	110 ± 8	35

[a]From this work. [b]No detectable change in absorbance after the addition of 100 equiv of 4-MeO-G.

DOI: 10.1021/acs.biochem.8b00540
Biochemistry XXXX, XXX, XXX−XXX

hydrophobic cavity surrounded by amino acids L100, F21, F24, F35, and V59) as determined from crystallographic studies of 4-halophenols binding to DHP.[60] When compared to the binding affinity of the known[42] DHP B inhibitor 4-Br-phenol (1.15 mM[56]), the 4-Br-guaiacol binding affinity is significantly stronger, which rationalizes the minimal impact this inhibitor had on 4-Br-guaiacol conversion (*vide supra*).

X-ray Crystallographic Studies of WT DHP B Complexed with Guaiacols. Crystal structures were determined to atomic resolution for DHP in complex with five different guaiacol substrates. X-ray data collection and refinement statistics are listed in Table S3, and selected distances are listed in Table 3. For each structure, WT DHP B

Table 3. Selected Distances (angstroms) for DHP B–Guaiacol Complexes (protomer A)[a]

	4-Br-G[b]	5-Br-G	6-Br-G[b]	4-NO_2-G	4-MeO-G
PDB entry	6CKE	6CRE	6CO5	6CH5	6CH6
substrate occupancy	90%	A, 35%/B, 30%	40%	70%[c]	75%
distal H_2O occupancy	100%	58%	34%	100%	90%
H55 N^{ε}···OH (guaiacol)	2.64^{int}	$2.47_A{}^{int}$/ $6.52_B{}^{ext}$	4.78^{ext}	2.61^{int}/ 8.35^{ext}	2.66^{int}/ 9.54^{ext}
H55 N^{δ}···OH (guaiacol)	4.62^{int}	$4.42_A{}^{int}$/ $5.51_B{}^{ext}$	6.38^{ext}	4.55^{int}/ 7.34^{ext}	4.65^{int}/ 7.55^{ext}
F21 C^{ζ}···C^1 (guaiacol)	3.76	4.17_A (C^2)/ 4.36_B (C^3)	4.05 (C^4)	3.71	3.73
F21 C^{γ}···C^4 (guaiacol)	3.97	3.67_A (C^5)/ 3.76_B (C^6)	3.71 (C^1)	3.78	3.93
Fe···OH (guaiacol)	4.85	4.78_A/7.28_B	6.75	4.75	4.74
Fe···O^{C2} (guaiacol)	4.62	4.71_A/6.08_B	6.96	4.71	4.68
Fe···X (guaiacol)	Br^{C4}, 8.43	Br^{C5}, 8.21_A/ 5.43_B	Br^{C6}, 5.61	N^{C4}, 8.04	O^{C4}, 7.85
^{guaiacol}OH··· distal H_2O	2.85	2.37_A	–	2.76	2.72
Fe···distal water	2.18	2.52	2.29	2.13	2.20
Fe···H55 N^{δ}	6.68	6.38^{int}/8.98^{ext}	6.54	6.44^{int}/ 8.80^{ext}	6.64^{int}/ 9.73^{ext}
Fe···H55 N^{ε}	6.01	5.84^{int}/ 10.17^{ext}	5.68	5.88^{int}/ 10.18^{ext}	5.91^{int}/ 11.59^{ext}
Fe···H89 N^{ε}	2.15	2.23	2.27	2.14	2.12
Fe to pyrrole N plane	0.062	0.063	0.062	0.059	0.059

[a]The two 5-Br-G conformations are denoted with subscripts A and B as shown in Figure 4B, and the two H55 conformations are designated as interior (int) or exterior (ext). [b]For 4-Br-G and 6-Br-G, H55 was found to be exclusively in the interior and exterior conformations, respectively. [c]4-NO_2-G also exhibited an additional slightly shifted conformation, but it is of minor occupancy and therefore not described.

crystallized with two molecules (A and B) per asymmetric unit, in agreement with all previously reported dehaloperoxidase crystal structures.[19] Each guaiacol substrate (4-Br-G, 5-Br-G, 6-Br-G, 4-NO_2-G, and 6-MeO-G) was found to bind in the distal pocket (Figure 4) with partial occupancy, sharing the distal pocket with a water molecule ligated to the heme Fe. As such, these DHP–guaiacol complexes are the first examples observed of ligand binding in DHP without the displacement of the distal water molecule. With the exception of 5-Br-G, all guaiacols exhibited a single binding site that was virtually identical for 4-Br-G (Figure 4A), 4-NO_2-G (Figure 4E), and 4-MeO-G (Figure 4D): the substrates were oriented for favorable π-stacking interactions with F21, their methoxy substituents were found in the Xe1 binding site (a hydrophobic cavity surrounded by amino acids L100, F21, F24, F35, and V59 that was shown to bind Xe),[60] the 4-X substituents (Br, NO_2, or MeO groups) were directed away from the heme in a hydrophobic region deeper in the distal cavity (reorienting F60 to accommodate the bulkier NO_2 and MeO substituents), and the phenolic OH for each was directed toward the heme Fe and within H-bonding distance of both H55 (N^{ε}) and the heme-bound distal water. Two conformations were observed for 5-Br-G, assigned as 5-Br-G_A and 5-Br-G_B: the binding orientation of 5-Br-G_A (Figure 4B) is similar to that of the 4-X-G (X = Br, NO_2, or MeO) binding sites; however, the Br atom resides closer to the cavity entrance. In addition, the 4-X-G molecules are better positioned for stronger π-stacking interactions with F21 than 5-Br-G_A, which is reflected in (i) the 4.6- and 1.3-fold stronger binding affinities of 4-Br-G and 4-NO_2-G, respectively, when compared to that of 5-Br-G and (ii) higher occupancies of the 4-X-G substrates compared to those of 5-Br-G (90% for 4-Br-G > 75% for 4-MeO-G > 70% for 4-NO_2-G > $35\%_A/30\%_B$ for 5-Br-G). In contrast, a rotation of the guaiacol molecule in the distal pocket was observed for 5-Br-G_B and 6-Br-G (panels B and C, respectively, of Figure 4), with the Br atoms located in the Xe1 binding site, the OH and methoxy groups oriented toward the top of the distal pocket, reduced π-stacking interactions with F21, and the unsubstituted region of the ring directed toward the heme cofactor. H55 is out of optimal H-bonding distance with regard to 5-Br-G_B (Table 3) yet is well-positioned to interact with the MeO oxygen of 6-Br-G.

As a side note, each guaiacol structure exhibited one of the two protomers in a bis-histidine-ligated (hexacoordinated) heme orientation (Figure 4F). We have previously[35] observed such a hemichrome species in DHP B when complexed with benzotriazole using crystals grown from PEG 4000 (as opposed to PEG 3350 here). Other DHP complexes (unpublished results) have exhibited the bis-histidine ligation in a single protomer when PEG 3350 was used, and as such, we surmise that this coordination can be attributed to the use of this precipitant during crystallization and is not exclusive to the guaiacol complexes. The functional consequences (if any) of the bis-histidine ligation were not further explored here.

Stopped-Flow UV–Vis Spectroscopic Studies with 4-Br-guaiacol. Single- and double-mixing stopped-flow UV–vis spectroscopic methods were used to investigate the reaction of 4-Br-guaiacol (as a representative 4-X-guaiacol substrate) with DHP B. Studies were performed with H_2O_2-activated DHP B {i.e., preformed as Compound I [DHP B(Y28F/Y38F)],[31] Compound ES,[32,40] or Compound II[41]} or by preincubating DHP B with 4-Br-guaiacol followed by addition of H_2O_2. For the majority of the studies described below, the data did not properly fit one-step, two species or two-step, three species irreversible mechanisms, and as such, experimentally obtained spectra at selected time points detailed in the figure legends are shown.

Compound I Reactivity. Generated in an initial mixing step of ferric DHP B (Y28F/Y38F) with 10 equiv of H_2O_2 in an aging line for 85 ms,[31] Compound I was reacted with 10 equiv of 4-Br-guaiacol at pH 7. The activated enzyme, Compound I [406 (Soret), 528, and 645 nm], was not observed (Figure 5A). Rather, ferric-like DHP B (Y28F/Y38F) [406 (Soret), 513, and 640 (sh) nm, black] was the first spectrum recorded,

DOI: 10.1021/acs.biochem.8b00540
Biochemistry XXXX, XXX, XXX–XXX

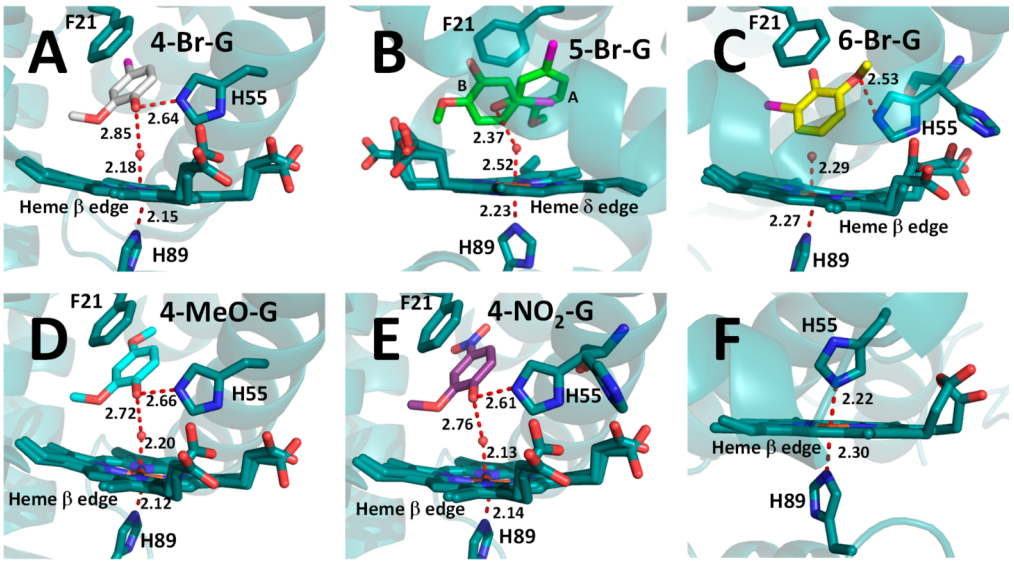

Figure 4. X-ray crystal structures of DHP B complexed with (A) 4-Br-guaiacol [gray, Protein Data Bank (PDB) entry 6CKE], (B) 5-Br-guaiacol (green, PDB entry 6CRE), (C) 6-Br-guaiacol (yellow, PDB entry 6CO5), (D) 4-methoxy-guaiacol (cyan, PDB entry 6CH6), and (E) 4-nitro-guaiacol (purple, PDB entry 6CH5). The Br atom for each substrate in panels A–C is colored magenta for the sake of clarity. (F) Bis-histidine hexacoordinated form of DHP.

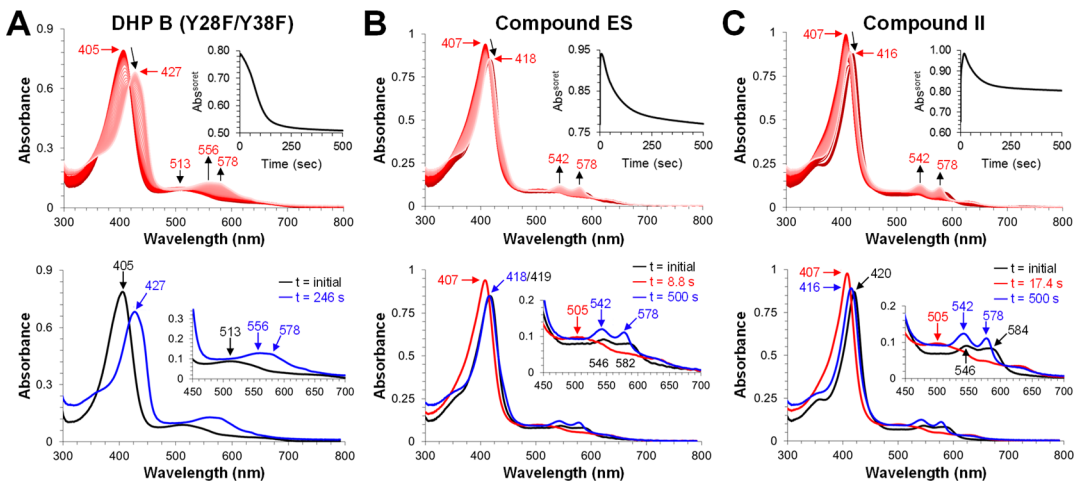

Figure 5. Kinetic data for the reaction of H_2O_2-activated DHP B with 4-Br-guaiacol. (A) DHP B (Y28F/Y38F). The top panel shows stopped-flow UV–vis spectra of the double-mixing reaction of preformed Compound I (10 μM) with a 10-fold excess of 4-Br-guaiacol at pH 7.0 (900 scans over 500 s). The inset shows the single-wavelength (408 nm) dependence on time obtained from the raw data. The bottom panel shows experimentally obtained spectra for Compound I reacted with 4-Br-guaiacol (black; t = 0 s), and its reduction to a ferrous-like species of DHP B was observed in the presence of 4-Br-guaiacol (blue; t = 246 s). (B) Ferric DHP B/Compound ES. The top panel shows stopped-flow UV–vis spectra of the double-mixing reaction of ferric DHP B (10 μM) premixed with 10 equiv of H_2O_2 (500 ms) and then reacted with 10 equiv of 4-Br-guaiacol at pH 7.0 (900 scans over 500 s). The inset shows the single-wavelength (408 nm) dependence on time obtained from the raw data. The bottom panel shows experimentally obtained spectra of Compound ES (black; t = 0 s) reacted with 4-Br-guaiacol, resulting in ferric DHP B (red; t = 8.8 s) and further reduction to oxyferrous DHP B (blue; t = 500 s). (C) Ferric DHP B/Compound II. The top panel shows stopped-flow UV–vis spectra of the single-mixing reaction between Compound II and 4-Br-guaiacol. Compound II was formed from an initial reaction between oxyferrous DHP B (10 μM) preincubated with 1 equiv of trichlorophenol and 10 equiv of H_2O_2 and reacted for 3 s prior to the second mixing with 4-Br-guaiacol at pH 7.0 (900 scans over 500 s). The inset shows the single-wavelength (408 nm) dependence on time obtained from the raw data. The bottom panel shows experimentally obtained spectra of Compound II (black; t = 0 s) reacted with 4-Br-guaiacol, resulting in ferric DHP B (red; t = 17.4 s) and further reduction to oxyferrous DHP B (blue; t = 246 s).

and it suggested that Compound I was reduced by the substrate within the mixing time (1.5 ms) of the stopped-flow apparatus. The rapid reaction of Compound I with 4-Br-guaiacol is virtually identical to its reactivity seen with 5-Br-indole,[24] 4-nitrophenol,[34] and pyrrole[25] in that these substrates could also reduce Compound I to the ferric enzyme within the stopped-flow mixing time. The ferric enzyme then converted to a new DHP B species [427 (Soret), 556, and 578 (sh) nm, blue; t = 246 s] that appeared to be a mixture of both ferrous and oxyferrous DHP.[41]

Compound ES Reactivity. Ferric WT DHP B was rapidly mixed with 10 equiv of H_2O_2 at pH 7, incubated for 500 ms to allow for the maximum accumulation of Compound ES (ferryl heme + tyrosyl radical),[40] and subsequently mixed with 10–50 equiv of 4-Br-guaiacol. As a representative reaction, the preformed Compound ES [418 (Soret), 546, and 582 nm,

DOI: 10.1021/acs.biochem.8b00540
Biochemistry XXXX, XXX, XXX–XXX

black; t = 0 s] was converted in the presence of 10 equiv of 4-Br-guaiacol to ferric DHP B [407 (Soret), 505, and 640 (sh) nm, red; t = 8.8 s] that underwent further reduction to the resting oxyferrous state after 500 s (Figure 5B and Table 4).

Table 4. Summary of Stopped-Flow UV−Vis Spectroscopic Data for the Reaction of Compound ES with Guaiacol Substrates at pH 7

substrate	Compound ES → ferric, time (s)	observed ferric species λ_{max} (nm)	ferric → oxyferrous, time (s)	final observed species λ_{max} (nm)
o-guaiacol	26	409, 504, 640	>500	411, 540, 578 (oxy/ferric mixture)
4-Br-G	9	407, 505, 640	>500	418, 542, 578 (oxy)
5-Br-G	5	411, 505, 640	n/a[a]	411, 505, 640 (Compound RH-like)
6-Br-G	n/o[b]	n/o[b]	n/o[b]	420, 455 (product)
4-NO_2-G	186	410, 539 (sh)	>500	412, 539, 576 (oxy/ferric mixture)
4-MeO-G	42	409, 503, 640	250	418, 543, 578 (oxy)
4-Me-G	30	409, 503, 640	n/a[a]	409, 503, 640 (Compound RH-like)

[a]n/a, not applicable (i.e., oxyferrous DHP was not formed). [b]n/o, not observable because of product formation at 455 nm.

The progression of the initial Compound ES reduction to the ferric enzyme, followed by a slower reduction to oxyferrous DHP, mirrors previous observations of Compound ES reactivity with haloindoles[24] and halophenols,[40] suggesting the similar product-driven reductions that occurred in those studies may also be present here with the guaiacol substrates.

Compound II Reactivity. Formed after 3 s in an aging line from an initial mixing step of 10 equiv of H_2O_2 with oxyferrous WT DHP B that was preincubated with 1 equiv of 2,4,6-trichlorophenol,[41] Compound II was reacted with 10 equiv of 4-Br-guaiacol. The preformed Compound II [420 (Soret), 546, and 584 nm, black; t = 0 s] initially converted to ferric DHP B [407 (Soret), 505, and 640 (sh) nm, red; t = 17.4 s], was further reduced to oxyferrous DHP B [416 (Soret), 542, and 578 (sh) nm, blue; t = 246 s] and remained stable as this species for the duration of the 500 s observation time (Figure 5C). The reduction of Compound II to ferric DHP by 4-Br-guaiacol here parallels the same observations made when employing TCP,[41] haloindole,[24] and pyrrole[25] substrates, as does the further reduction (presumably product-driven) to oxyferrous DHP; albeit virtually complete formation (in lieu of a ferric/oxyferrous DHP mixture) was observed here (*vide infra*).

Oxyferrous Reactivity. It has been previously shown that oxyferrous DHP can be activated by H_2O_2 in the presence of halophenol,[41,61,62] haloindole,[24] and pyrrole[25] substrates, whereas in their absence, only a slight bleaching of the Soret band and/or long time scale conversion to Compound RH is observed. To investigate if guaiacols can facilitate this substrate-dependent activation of DHP, stopped-flow methods were employed to rapidly mix H_2O_2 (10 equiv) with a solution of oxyferrous DHP B that was preincubated with 10 equiv of 4-Br-guaiacol. The following spectral changes were noted: oxyferrous DHP B [416 (Soret), 542, and 578 nm, black; t = 0 s] was oxidized to ferric DHP B [407 (Soret), 501, and 640 (sh) nm, red; t = 7.3 s], followed by a gradual reduction back to the oxyferrous state [413 (Soret), 541, and 578 nm, blue; t = 500 s] (Figure S6). Interestingly, no transiently observed ferryl species were formed, which differs from the reaction performed in the presence of halophenol,[41] haloindole,[24] and pyrrole[25] substrates where the Compound II intermediate was observed.

Double-mixing stopped-flow UV−vis spectroscopic methods were also used to investigate the reactivity of the remaining guaiacol substrates (10−50 equiv) with preformed Compound ES in a manner identical to that described above for 4-Br-guaiacol. Figures S7 and S8 display representative reactions of preformed Compound ES [418 (Soret), 546, and 582 (sh) nm, black; t = 0 s] with 10 equiv of each of the guaiacol substrates, and Table 4 summarizes the optical data. Although the time required to do so varied >40-fold (4.37−186 s), all substrates were found to reduce Compound ES to ferric DHP B. However, while four (*o*-guaiacol, 4-Br-G, 4-MeO-G, and 4-NO_2-G) of the seven guaiacol reactions were found to further reduce the resultant ferric enzyme to the oxyferrous state, two were unable to do so: 4-Me-guaiacol (Figure S8A) and 5-Br-guaiacol (Figure S8B). Rather, the enzyme converted to a mixture of ferric DHP and the peroxidase-attenuated state Compound RH.[31,32,40] Importantly, the formation of oxyferrous DHP in these stopped-flow studies strongly correlated with the observation of 2-MeOBQ as identified in the HPLC studies described above, suggesting that 2-MeOBQ could serve as a reducing agent of ferric DHP (*vide infra*). In the case of 6-Br-guaiacol (Figure S8C), the formation of a product that exhibited a strong absorption band at ∼450 nm that overlapped with the Soret and Q bands prevented any conclusive spectral assignments.

The main observations from these stopped-flow studies were as follows. (i) The H_2O_2-activated enzyme was reduced to ferric DHP by 4-Br-guaiacol, with the rate of reduction decreasing in the following order: Compound I > Compound ES > Compound II. (ii) The oxyferrous enzyme reacted with H_2O_2 in the presence of 4-Br-guaiacol, however without the formation of an observable Compound II species. (iii) All of the reactions with 4-Br-guaiacol yielded oxyferrous DHP as a final observable species. (iv) 2-MeOBQ was identified as the putative reductant.

Reduction of Ferric DHP B by 2-MeOBQ. Stopped-flow UV−vis spectroscopic methods were employed to explore if the 2-MeOBQ product was capable of the aerobic reduction of ferric DHP to yield the oxyferrous enzyme observed in the studies mentioned above. A solution of 8 μM ferric DHP B was rapidly mixed with authentic 2-MeOBQ [62.5 μM (Figure 6); 0.625, 6.25, and 625 μM (Figure S9)] at pH 7 and monitored for 50 s. For 2-MeOBQ concentrations of 6.25−625 μM, the data were best fit to a two-step, three-species irreversible mechanism: the first step (k_1) yielded an initial oxyferrous-like species whose spectral features were similar, but not identical, to those of oxyferrous DHP B [UV−vis spectrum 419−20 (Soret), 542−544, and 578 nm] that was subsequently fully formed in the second step (k_2). Interestingly, the reaction exhibited saturable kinetics with respect to k_1 and 2-MeOBQ, whereas k_2 was independent of the 2-MeOBQ concentration (Figure S10). Even at a substoichiometric concentration of 0.625 μM 2-MeOBQ (Figure S9A), a partial formation of oxyferrous DHP was observed. Overall, the reduction observed

DOI: 10.1021/acs.biochem.8b00540
Biochemistry XXXX, XXX, XXX−XXX

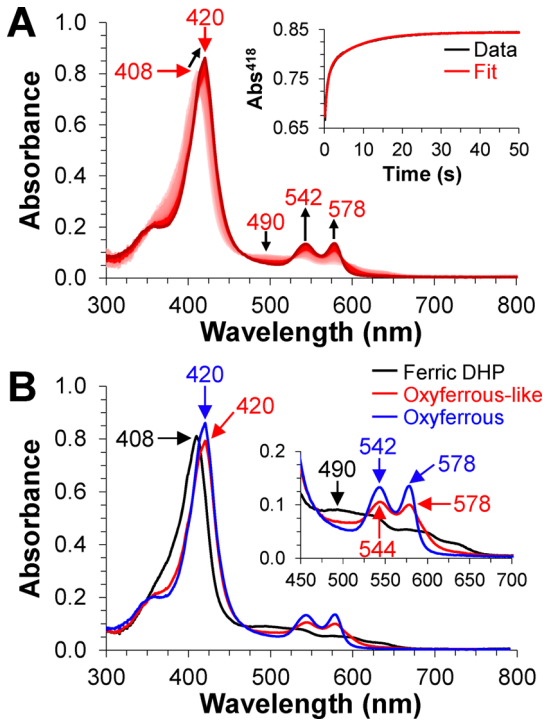

Figure 6. Kinetic data for the reaction of 2-MeOBQ with ferric DHP B. (A) Stopped-flow UV−vis spectra of the single-mixing reaction of ferric DHP B (10 μM) reacted with 62.5 μM 2-MeOBQ at pH 7.0 (900 scans over 50 s). The inset shows the single-wavelength (418 nm) dependence on time obtained from the raw data (black) and the corresponding fit (red). (B) Calculated spectra of the three reaction components derived from the SVD analysis: ferric DHP B (black), an apparent mixture of ferric and oxyferrous DHP B (red), and oxyferrous DHP B (blue).

here with 2-MeOBQ was appreciably faster than that observed previously with 2,6-dichloro-1,4-dibenzoquinone (for DCQ, k_{obs} = 0.085 s^{-1}),[40] which is the product of the DHP-catalyzed oxidative dehalogenation of 2,4,6-trichlorophenol. These results support a "product-driven" reduction wherein the 2-MeOBQ product of guaiacol oxidation via a DHP peroxidase activity reduces the peroxidase-active ferric DHP B to its hemoglobin-active oxyferrous state.

DISCUSSION

The activity studies reported here demonstrate that DHP B could catalyze the conversion of all guaiacols studied under physiological conditions. With the exception of *o*-guaiacol that had an only 70% conversion to products, both monosubstituted native-halogenated guaiacols (-F, -Cl, and -Br) and nonnative guaiacols (-Me, -OMe, and -NO_2) were converted in high yields (>90%) to monomeric and oligomeric product(s). Isotopic labeling studies unequivocally demonstrated that the oxygen atom incorporated into the products for the 4-Br-guaiacol reaction originated exclusively from H_2O, while radical scavengers were shown to inhibit substrate conversion. Together, these results provide support for the idea that guaiacol oxidation follows a radical-based peroxidase mechanism. Moreover, the oxidation of the guaiacol substrates could be initiated from either the traditional peroxidase ferric oxidation state or the oxyferrous form of the enzyme that is relevant to the O_2-transport function of DHP as the coelomic hemoglobin of *A. ornata*.

These results are consistent with the well-established peroxidase activity of DHP B with trihalophenol substrates[11] and with previous studies of guaiacol oxidation by other peroxidase enzymes, specifically myoglobin and other heme peroxidases, in which it has been used as a classic substrate in kinetic assays because of the formation of the highly colored (λ_{max} = 470 nm) 3,3′-dimethoxy-4,4′-biphenoquinone reaction product.[58,63] Some notable examples of guaiacol oxidation in these systems include (i) monitoring the peroxidase activity of myoglobin mutants via guaiacol oxidation[64−66] and (ii) the oxidation of guaiacol by horseradish peroxidase,[57,59] lignin peroxidase,[10] and manganese peroxidase.[67] In those systems, the products were identified as guaiacol dimers (i.e., 3,3′-dimethoxy-4,4′-biphenoquinone and its reduced analogue, 3,3′-dimethoxy-4,4′-diphenol), trimers, and tetramers, with the guaiacol moieties linked through the carbon *ortho* to the phenol group.[57] The monomer, 2-MeOBQ, however was not observed in those studies, but it has been previously identified in the case of laccase-catalyzed phenol dehydrogenation[68] and in studies of guaiacol oxidation employing small molecule catalysts (i.e., silver oxide, ferric chloride, and chromium trioxide).[69,70] The results presented herein demonstrate that DHP B is capable of oxidizing 4-R-guaiacols (with the exception of R = Me) to 2-MeOBQ, either as the major product (R = F, Cl, or Br) or as a minor product (R = H, MeO, or NO_2).

The formation of 2-MeOBQ further establishes the "product-driven" reduction observed in DHP that appears to be a hallmark of this catalytic hemoglobin. At 206 ± 6 mV,[40] the Fe^{III}/Fe^{II} redox couple for DHP B is higher than most other hemoglobins (e.g., human Hb, 158 mV;[71] horse heart Hb, 152 mV;[72] horse heart Mb, 46 mV;[73] sperm whale Mb, −43 mV[74]) and significantly more so than other peroxidases (e.g., myeloperoxidase, −5 mV;[75] cytochrome *c* peroxidase, −182 mV;[76] HRP, −266 mV[77]). Demonstrated first with 2,6-dichloroquinone (DCQ),[40] the oxidation product of its peroxidase activity with 2,4,6-trichlorophenol, and later with 5-Br-3-oxindole,[24] the oxidation product of its peroxygenase activity with 5-Br-indole, DHP has been shown (almost counterintuitively) to be susceptible to reduction by the oxidation products of its catalytic activities. Here, we provide strong evidence that the "product-driven" reduction can be attributed to 2-MeOBQ, which may serve as a "rescue" of the enzyme to return to its oxyferrous state, thereby enabling this multifunctional hemoglobin to maintain its O_2-transport function after cycling peroxidase activity.

Importantly, activation of oxyferrous DHP in the presence of a guaiacol substrate and H_2O_2 was also demonstrated, suggesting that the entire catalytic cycle can be initiated from, and ultimately return to, the hemoglobin-active O_2 carrier state. How such a substrate-dependent activation of oxyferrous DHP occurs has been the subject of several studies, and two possible mechanisms have been suggested. (i) Trace amounts of the ferric enzyme react with H_2O_2 and the substrate, thereby generating diffusible substrate radicals that oxidize oxyferrous DHP to the catalytically active ferric form,[61,62] or (ii) substrate binding to DHP destabilizes the oxyferrous state in the presence of hydrogen peroxide, leading to a reaction between ferrous DHP and H_2O_2 that activates the enzyme via a Compound II intermediate that is subsequently quickly reduced to the ferric enzyme.[41] Here, we employed the spin trap 5,5-dimethyl-1-pyrroline *N*-oxide (DMPO) to scavenge diffusible radicals and noted that the 4-Br-guaiacol

DOI: 10.1021/acs.biochem.8b00540
Biochemistry XXXX, XXX, XXX−XXX

reaction was unaffected by DMPO, giving the same substrate conversion and 2-MeOBQ product formation observed in its absence. Accordingly, these data suggest that the reaction of 4-Br-guaiacol does not generate a diffusible radical species and, although they are not directly supportive of an oxyferrous destabilization mechanism, appear to rule out the one involving diffusible substrate radicals. However, as both 5-Br-G and 4-NO_2-G exhibited reduced substrate conversion in the presence of the spin trap, we cannot rule out a substrate radical-based oxyferrous activation mechanism for these substrates.

The lack of an effect by DMPO on 4-Br-guaiacol reactivity suggests that either two successive one-electron oxidation steps[78] occur without the substrate radical diffusing out of the active site or a single two-electron oxidation occurs. The question of why oxidation via electron transfer is preferred with guaiacol substrates, as opposed to O atom transfer, given that DHP is capable of both thus arises. To address this, we turn to the X-ray crystallographic studies to provide insight. 4-Br-G, 5-Br-G_A, 4-NO_2-G, and 4-MeO-G bind near the α-edge of the heme cofactor (Figure 7, panels A and B), similar to other

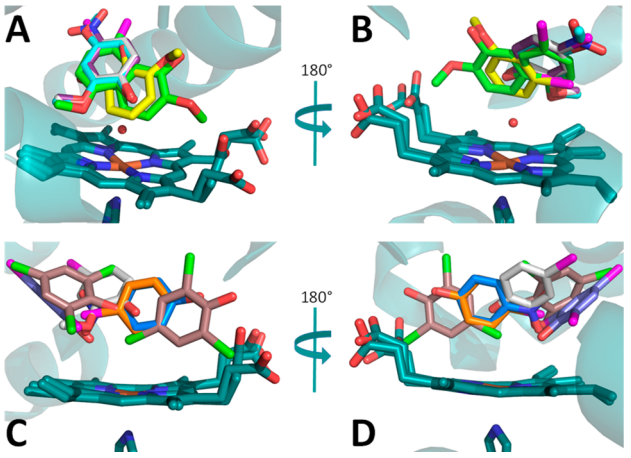

Figure 7. Superposition of selected DHP substrates. Guaiacol binding site superposition provided in panels A and B for 4-Br-G (silver, PDB entry 4CKE), 5-Br-G (green, PDB entry 5CRE), 6-Br-G (yellow, PDB entry 6CO5), 4-NO_2-G (purple, PDB entry 6CH5), and 4-MeO-G (cyan, PDB entry 6CH6). Panels C and D provide the superposition of 4-Br-G (silver) with peroxidase substrates TBP (purple, PDB entry 4FH6[79]) and TCP (brown, PDB entries 4KMW and 4KMV[27]), peroxygenase substrate 4NP (blue, PDB entry 5CHQ[34]), and inhibitor 4BP (orange, PDB entry 3LB2[56]).

peroxidase substrates, i.e., TBP[79] and one of the two TCP[27] sites (Figure 7, panels C and D). In the context of the comparisons shown in Figure 1, the X-ray crystal structures demonstrate the following. (i) When compared to the peroxygenase substrate 4-nitrophenol (4-NP) binding site (Figure 7, panels C and D, blue),[34] which is positioned close to the heme center in an orientation that allows for direct O atom transfer from the activated ferryl intermediate, the 4-Br-G, 5-Br-G_A, 4-NO_2-G, and 4-MeO-G binding sites are farther from the heme Fe that is not conducive to O atom transfer. (ii) When compared to the 4-Br-phenol inhibitor site (Figure 7, panels C and D, orange) that binds directly above the heme-Fe in a manner that likely inhibits H_2O_2 activation, 4-Br-G resides farther from the heme face, allowing for H_2O_2 binding and subsequent catalytic activity. (iii) Although the structure of the DHP–*o*-guaiacol complex was not obtained, we can surmise either that it likely binds in a fashion nearly identical to that of 4-Br-G or that the methoxy substituent reorients to occupy the Xe1 site, either of which would preclude O atom transfer on the basis of distance arguments. Finally, the crystal structures also demonstrate that the hypothetical site of oxygen atom insertion (i.e., the phenol ring carbon closest to the activated heme) is sterically hindered by the methoxy group itself, thus precluding oxygen atom transfer and supporting oxidation via electron transfer (i.e., a peroxidase mechanism). Interestingly, the guaiacol substrates that share a common binding motif, i.e., 4-Br-G, 4-NO_2-G, and 4-MeO-G (and presumably including 4-F-G and 4-Cl-G whose structures were not determined but are likely similar to that of the brominated analogue), all form 2-MeOBQ as their primary oxidation product. Taken together, the methoxy substituent appears to play a role in positioning the guaiacol substrate for oxidation via electron (but not O atom) transfer, with the substitution pattern on the phenol ring (4-X vs 5/6-X) also dictating product outcome.

On the basis of the results described above, and through previously established mechanisms for peroxidases (including dehaloperoxidase[19,21,40] and more traditional ones such as HRP[80]), we propose the following catalytic cycle for the *in vitro* hydrogen peroxide-dependent oxidation of guaiacols by DHP (Scheme 1). Ferric DHP B reacts with 1 equiv of H_2O_2 forming a two-electron oxidized ferryl species (step i-a), either as Compound I[31] or as Compound ES,[40] which is subsequently

Scheme 1. Proposed Catalytic Cycle for the Oxidation of 4-X-Guaiacols by DHP B

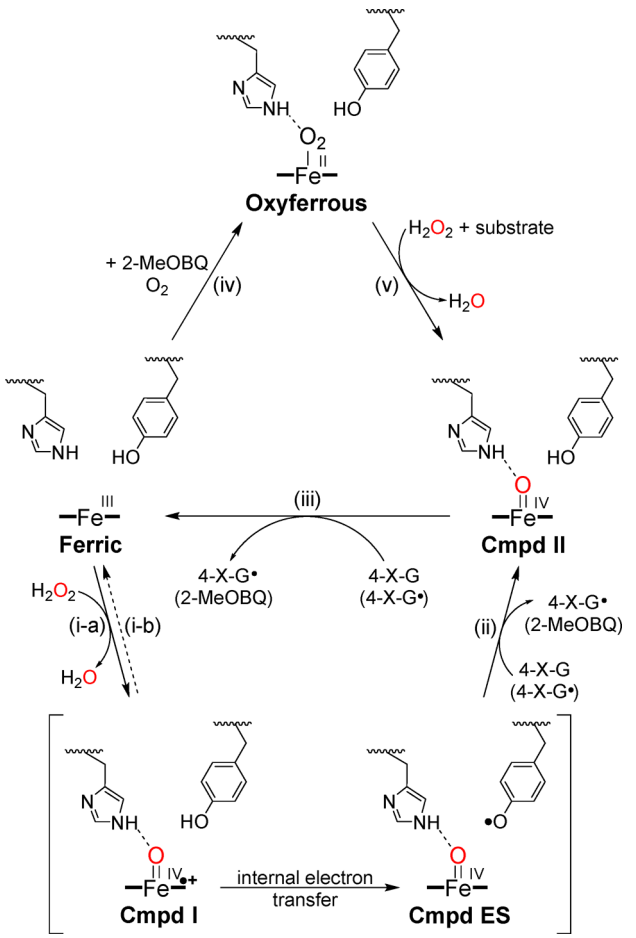

DOI: 10.1021/acs.biochem.8b00540
Biochemistry XXXX, XXX, XXX–XXX

reduced in the presence of a guaiacol substrate to the ferric enzyme, yielding 2-MeOBQ. This can occur in one of two ways. The first possibility is through two consecutive one-electron oxidations[78] of 4-X-guaiacol (steps ii and iii), wherein 2-MeOBQ can form via a diffusible phenoxy 4-X-G$^{\bullet}$ radical that is subsequently oxidized by activated DHP or through the disproportionation[81] of two 4-X-G$^{\bullet}$ radicals. The formation of diffusible radicals is consistent with radical−radical coupling reactions that account for the observed higher-molecular weight products [i.e., dimers, trimers, etc. (Table S1 and Table S2)] as these are unable to form within the steric constraints of the DHP active site. The second possibility is via a direct two-electron oxidation (step i-b), i.e., in the case of 4-Br-guaiacol, where 2-MeOBQ formation occurs without a diffusible substrate radical, a result that is consistent both with the lack of observed higher-molecular weight species that are derived from radical−radical recombination and with the lack of an effect on product yield when employing the radical quencher DMPO. Regardless of which pathway results in its formation, the 2-MeOBQ product reduces ferric DHP aerobically to the oxyferrous form of the enzyme (step iv), which itself can be activated for peroxidase function in the presence of H_2O_2 and the guaiacol substrate, presumably through a Compound II species (step v). These latter two steps highlight the versatility of DHP as a catalytic hemoglobin in that the resting form of the enzyme can be the O_2-transport oxyferrous state, which is typically inactive for monofunctional peroxidases.[82]

CONCLUSION

In summary, the addition of an electron-donating methoxy group to phenolic substrates has a profound effect on their DHP-mediated oxidation. 4-Br-guaiacol and 4-NO_2-guaiacol are clearly peroxidase substrates, whereas 4-Br-phenol (inhibitor) and 4-NO_2-phenol (peroxygenase substrate) are not. We have previously[24,25,34] suggested that the substrate itself can act to modulate enzyme activity in DHP, with binding/orientation (relative to the ferryl iron), pK_a, and redox potential all being key determinants of which DHP mechanism leads to substrate oxidation. With the addition of the guaiacol substrates studied here, we have further established that substituent effects may also play a role, with electron-withdrawing groups appearing to favor peroxygenase activity, while electron-donating groups promote oxidation via a peroxidase mechanism, with discrimination between the two likely being a function of substrate binding distance and/or (de)stabilization of the one-electron oxidized substrate radical. In a broader sense, these substituent effects suggest that it may be possible to further tune DHP activity, not just through traditional mutagenesis or heme cofactor modification but through selection of the substrate itself. Regardless, the results also demonstrate that critical to it being a multifunctional globin, DHP-catalyzed guaiacol oxidation can be initiated from the oxyferrous state, cycle through a peroxidase mechanism, and undergo a product-driven reduction, thereby returning the enzyme to its O_2 carrier state. As such, the combination of a substrate-dependent structure−function activity and unique product-driven reduction provides a mechanism by which DHP can act both as a hemoglobin (O_2 transport) and as a detoxification enzyme for survival against small molecule toxins.

ASSOCIATED CONTENT

Supporting Information

The Supporting Information is available free of charge on the ACS Publications website at DOI: 10.1021/acs.biochem.8b00540.

HPLC chromatograms, LC−MS studies, titration curves, and stopped-flow data for the reaction of DHP with guaiacol substrates and X-ray data collection and refinement statistics for DHP in complex with 4-Br-G, 5-Br-G, 6-Br-G, 4-NO_2-G, and 4-MeO-G (PDF)

AUTHOR INFORMATION

Corresponding Author

*Department of Chemistry, North Carolina State University, Raleigh, NC 27695. E-mail: Reza_Ghiladi@ncsu.edu. Phone: (919) 513-0680. Fax: (919) 515-8920.

ORCID

Reza A. Ghiladi: 0000-0002-6450-9311

Funding

This project was supported by National Science Foundation CAREER Award CHE-1150709, CHE-1609446, and Research Experience for Undergraduates CHE-1659690.

Notes

The authors declare no competing financial interest.

ACKNOWLEDGMENTS

The authors gratefully acknowledge Prof. Stefan Franzen (North Carolina State University) for helpful discussions regarding DHP structure−activity relationships. Mass spectra were recorded at the Mass Spectrometry Facility for Biotechnology at North Carolina State University. Partial funding for the facility was obtained from the North Carolina Biotechnology Center and the National Science Foundation. X-ray diffraction data were collected at Southeast Regional Collaborative Access Team (SER-CAT) beamline 22-BM at the Advanced Photon Source, Argonne National Laboratory. Supporting institutions may be found at www.ser-cat.org/members.html. Use of the Advanced Photon Source was supported by the U.S. Department of Energy, Office of Science, Office of Basic Energy Sciences, under Contract W-31-109-Eng-38.

ABBREVIATIONS

2,4-DNP, 2,4-dinitrophenol; 2-MeOBQ, 2-methoxy-1,4-benzoquinone; 4-Br-G, 4-bromoguaiacol; 4-BP, 4-bromophenol; 4-Cl-G, 4-chloroguaiacol; 4-F-G, 4-fluoroguaiacol; 4-MeO-G, 4-methoxyguaiacol; 4-Me-G, 4-methylguaiacol; 4-NO_2-G, 4-nitroguaiacol; 4-NP, 4-nitrophenol; 5-Br-G, 5-bromoguaiacol; DMPO, 5,5-dimethyl-1-pyrroline *N*-oxide; 6-Br-G, 6-bromoguaiacol; Compound I, two-electron-oxidized heme cofactor compared to the ferric form, commonly as an Fe^{IV}=O porphyrin π-cation radical; Compound II, one-electron-oxidized heme cofactor compared to the ferric form, commonly as an Fe^{IV}=O or Fe^{IV}−OH compound; Compound ES, two-electron-oxidized state containing both a ferryl center (Fe^{IV}=O) and an amino acid (tryptophanyl or tyrosyl) radical, analogous to Compound ES in cytochrome *c* peroxidase; Compound RH, "reversible heme" state of dehaloperoxidase, formed from the decay of Compound ES in the absence of a co-substrate; DHP, dehaloperoxidase; Hb,

DOI: 10.1021/acs.biochem.8b00540
Biochemistry XXXX, XXX, XXX−XXX

hemoglobin; HSM, horse skeletal muscle; Mb, myoglobin; TBP, 2,4,6-tribromophenol; TCP, 2,4,6-trichlorophenol.

REFERENCES

(1) Pokhrel, D., and Viraraghavan, T. (2004) Treatment of pulp and paper mill wastewater—a review. *Sci. Total Environ. 333*, 37−58.

(2) Samet, Y., Ayadi, M., and Abdelhedi, R. (2009) Degradation of 4-Chloroguaiacol by Dark Fenton and Solar Photo-Fenton Advanced Oxidation Processes. *Water Environ. Res. 81*, 2389−2397.

(3) Samet, Y., Wali, I., and Abdelhédi, R. (2011) Kinetic degradation of the pollutant guaiacol by dark Fenton and solar photo-Fenton processes. *Environ. Sci. Pollut. Res. 18*, 1497.

(4) Kroflič, A., Grilc, M., and Grgić, I. (2015) Unraveling Pathways of Guaiacol Nitration in Atmospheric Waters: Nitrite, A Source of Reactive Nitronium Ion in the Atmosphere. *Environ. Sci. Technol. 49*, 9150−9158.

(5) Agarwal, V., El Gamal, A. A., Yamanaka, K., Poth, D., Kersten, R. D., Schorn, M., Allen, E. E., and Moore, B. S. (2014) Biosynthesis of polybrominated aromatic organic compounds by marine bacteria. *Nat. Chem. Biol. 10*, 640.

(6) Larachi, F., Leroux, M., Hamoudi, S., Bernis, A., and Sayari, A. (2000) Solubility and Infinite Dilution Activity Coefficient for 5-Chlorovanillin and 4-Chloroguaiacol in Water over the Temperature Range 280 to 363 K. *J. Chem. Eng. Data 45*, 404−408.

(7) Kroflič, A., Grilc, M., and Grgić, I. (2015) Does toxicity of aromatic pollutants increase under remote atmospheric conditions? *Sci. Rep. 5*, 8859.

(8) Lauraguais, A., Coeur-Tourneur, C., Cassez, A., Deboudt, K., Fourmentin, M., and Choël, M. (2014) Atmospheric reactivity of hydroxyl radicals with guaiacol (2-methoxyphenol), a biomass burning emitted compound: Secondary organic aerosol formation and gas-phase oxidation products. *Atmos. Environ. 86*, 155−163.

(9) Pflieger, M., and Kroflič, A. (2017) Acute toxicity of emerging atmospheric pollutants from wood lignin due to biomass burning. *J. Hazard. Mater. 338*, 132−139.

(10) Koduri, R. S., and Tien, M. (1995) Oxidation of Guaiacol by Lignin Peroxidase: Role of Veratryl Alcohol. *J. Biol. Chem. 270*, 22254−22258.

(11) Ihssen, J., Jankowska, D., Ramsauer, T., Reiss, R., Luchsinger, R., Wiesli, L., Schubert, M., Thöny-Meyer, L., and Faccio, G. (2017) Engineered Bacillus pumilus laccase-like multi-copper oxidase for enhanced oxidation of the lignin model compound guaiacol. *Protein Eng., Des. Sel. 30*, 449−453.

(12) Chen, M., Qin, X., and Zeng, G. (2016) Single-walled carbon nanotube release affects the microbial enzyme-catalyzed oxidation processes of organic pollutants and lignin model compounds in nature. *Chemosphere 163*, 217−226.

(13) Nnamchi, C. I., Parkin, G., Efimov, I., Basran, J., Kwon, H., Svistunenko, D. A., Agirre, J., Okolo, B. N., Moneke, A., Nwanguma, B. C., Moody, P. C. E., and Raven, E. L. (2016) Structural and spectroscopic characterisation of a heme peroxidase from sorghum. *JBIC, J. Biol. Inorg. Chem. 21*, 63−70.

(14) Miner, K. D., Pfister, T. D., Hosseinzadeh, P., Karaduman, N., Donald, L. J., Loewen, P. C., Lu, Y., and Ivancich, A. (2014) Identifying the Elusive Sites of Tyrosyl Radicals in Cytochrome c Peroxidase: Implications for Oxidation of Substrates Bound at a Site Remote from the Heme. *Biochemistry 53*, 3781−3789.

(15) Hu, X., Wang, C., Wang, L., Zhang, R., and Chen, H. (2014) Influence of temperature, pH and metal ions on guaiacol oxidation of purified laccase from Leptographium qinlingensis. *World J. Microbiol. Biotechnol. 30*, 1285−1290.

(16) Morales, M., Mate, M. J., Romero, A., Martínez, M. J., Martínez, Á. T., and Ruiz-Dueñas, F. J. (2012) Two Oxidation Sites for Low Redox Potential Substrates: A Directed Mutagenesis, Kinetic, and Crystallographic Study on *Pleurotus Eryngii* Versatile Peroxidase. *J. Biol. Chem. 287*, 41053−41067.

(17) Pollock, L. (1998) *A Practical Guide to the Marine Animals of Northeastern North America*, Rutgers University Press, New Brunswick, NJ.

(18) Gribble, G. W. (2010) *Naturally Occurring Organohalogen Compounds: A Comprehensive Update*, Vol. *91*, Springer, Vienna.

(19) Franzen, S., Ghiladi, R. A., Lebioda, L., and Dawson, J. (2016) Multi-functional Hemoglobin Dehaloperoxidases. In *Heme Peroxidases*, Chapter 10, pp 218−244, The Royal Society of Chemistry.

(20) Lebioda, L., LaCount, M. W., Zhang, E., Chen, Y. P., Han, K., Whitton, M. M., Lincoln, D. E., and Woodin, S. A. (1999) An enzymatic globin from a marine worm. *Nature 401*, 445.

(21) Franzen, S., Thompson, M. K., and Ghiladi, R. A. (2012) The dehaloperoxidase paradox. *Biochim. Biophys. Acta, Proteins Proteomics 1824*, 578−588.

(22) Weber, R. E., Mangum, C., Steinman, H., Bonaventura, C., Sullivan, B., and Bonaventura, J. (1977) Hemoglobins of two terebellid polychaetes: *Enoplobranchus sanguineus and Amphitrite ornata*. *Comp. Biochem. Physiol. A Comp. Physiol. 56*, 179−187.

(23) LaCount, M. W., Zhang, E., Chen, Y. P., Han, K., Whitton, M. M., Lincoln, D. E., Woodin, S. A., and Lebioda, L. (2000) The crystal structure and amino acid sequence of dehaloperoxidase from *Amphitrite ornata* indicate common ancestry with globins. *J. Biol. Chem. 275*, 18712−18716.

(24) Barrios, D. A., D'Antonio, J., McCombs, N. L., Zhao, J., Franzen, S., Schmidt, A. C., Sombers, L. A., and Ghiladi, R. A. (2014) Peroxygenase and oxidase activities of dehaloperoxidase-hemoglobin from *Amphitrite ornata*. *J. Am. Chem. Soc. 136*, 7914−7925.

(25) McCombs, N. L., Smirnova, T., and Ghiladi, R. A. (2017) Oxidation of Pyrrole by Dehaloperoxidase-Hemoglobin: Chemoenzymatic Synthesis of Pyrrolin-2-Ones. *Catal. Sci. Technol. 7*, 3104−3118.

(26) Sun, S., Sono, M., Wang, C., Du, J., Lebioda, L., and Dawson, J. H. (2014) Influence of heme environment structure on dioxygen affinity for the dual function *Amphitrite ornata* hemoglobin/dehaloperoxidase. Insights into the evolutional structure−function adaptations. *Arch. Biochem. Biophys. 545*, 108−115.

(27) Wang, C., Lovelace, L. L., Sun, S., Dawson, J. H., and Lebioda, L. (2013) Complexes of dual-function hemoglobin/dehaloperoxidase with substrate 2,4,6-trichlorophenol are inhibitory and indicate binding of halophenol to compound I. *Biochemistry 52*, 6203−6210.

(28) Du, J., Huang, X., Sun, S., Wang, C., Lebioda, L., and Dawson, J. H. (2011) Amphitrite ornata Dehaloperoxidase (DHP): Investigations of Structural Factors That Influence the Mechanism of Halophenol Dehalogenation Using "Peroxidase-like" Myoglobin Mutants and "Myoglobin-like" DHP Mutants. *Biochemistry 50*, 8172−8180.

(29) Carey, L. M., Gavenko, R., Svistunenko, D. A., and Ghiladi, R. A. (2018) How nature tunes isoenzyme activity in the multifunctional catalytic globin dehaloperoxidase from Amphitrite ornata. *Biochim. Biophys. Acta, Proteins Proteomics 1866*, 230−241.

(30) Carey, L. M., Kim, K. B., McCombs, N. L., Swartz, P., Kim, C., and Ghiladi, R. A. (2018) Selective tuning of activity in a multifunctional enzyme as revealed in the F21W mutant of dehaloperoxidase B from Amphitrite ornata. *JBIC, J. Biol. Inorg. Chem. 23*, 209−219.

(31) Dumarieh, R., D'Antonio, J., Deliz-Liang, A., Smirnova, T., Svistunenko, D. A., and Ghiladi, R. A. (2013) Tyrosyl Radicals in Dehaloperoxidase: How nature deals with evolving an oxygen-binding globin to a biologically relevant peroxidase. *J. Biol. Chem. 288*, 33470−33482.

(32) Thompson, M. K., Franzen, S., Ghiladi, R. A., Reeder, B. J., and Svistunenko, D. A. (2010) Compound ES of dehaloperoxidase decays via two alternative pathways depending on the conformation of the distal histidine. *J. Am. Chem. Soc. 132*, 17501−17510.

(33) Feducia, J., Dumarieh, R., Gilvey, L. B., Smirnova, T., Franzen, S., and Ghiladi, R. A. (2009) Characterization of dehaloperoxidase compound ES and its reactivity with trihalophenols. *Biochemistry 48*, 995−1005.

(34) McCombs, N. L., D'Antonio, J., Barrios, D. A., Carey, L. M., and Ghiladi, R. A. (2016) Nonmicrobial Nitrophenol Degradation via Peroxygenase Activity of Dehaloperoxidase-Hemoglobin from *Amphitrite ornata*. *Biochemistry 55*, 2465−2478.

DOI: 10.1021/acs.biochem.8b00540
Biochemistry XXXX, XXX, XXX−XXX

(35) McCombs, N. L., Moreno-Chicano, T., Carey, L. M., Franzen, S., Hough, M. A., and Ghiladi, R. A. (2017) Interaction of Azole-Based Environmental Pollutants with the Coelomic Hemoglobin from Amphitrite ornata: A Molecular Basis for Toxicity. *Biochemistry 56*, 2294−2303.
(36) Han, K., Woodin, S. A., Lincoln, D. E., Fielman, K. T., and Ely, B. (2001) Amphitrite ornata, a marine worm, contains two dehaloperoxidase genes. *Mar. Biotechnol. 3*, 287−292.
(37) de Serrano, V., D'Antonio, J., Franzen, S., and Ghiladi, R. A. (2010) Structure of dehaloperoxidase B at 1.58 A resolution and structural characterization of the AB dimer from *Amphitrite ornata*. *Acta Crystallogr., Sect. D: Biol. Crystallogr. 66*, 529−538.
(38) Poulos, T. L., and Kraut, J. (1980) The stereochemistry of peroxidase catalysis. *J. Biol. Chem. 255*, 8199−8205.
(39) Davydov, R., Osborne, R. L., Shanmugam, M., Du, J., Dawson, J. H., and Hoffman, B. M. (2010) Probing the oxyferrous and catalytically active ferryl states of *Amphitrite ornata* dehaloperoxidase by cryoreduction and EPR/ENDOR spectroscopy. Detection of compound I. *J. Am. Chem. Soc. 132*, 14995−15004.
(40) D'Antonio, J., D'Antonio, E. L., Thompson, M. K., Bowden, E. F., Franzen, S., Smirnova, T., and Ghiladi, R. A. (2010) Spectroscopic and mechanistic investigations of dehaloperoxidase B from *Amphitrite ornata*. *Biochemistry 49*, 6600−6616.
(41) D'Antonio, J., and Ghiladi, R. A. (2011) Reactivity of deoxy- and oxyferrous dehaloperoxidase B from *Amphitrite ornata*: Identification of compound II and its ferrous-hydroperoxide precursor. *Biochemistry 50*, 5999−6011.
(42) Zhao, J., and Franzen, S. (2013) Kinetic study of the inhibition mechanism of dehaloperoxidase-hemoglobin a by 4-bromophenol. *J. Phys. Chem. B 117*, 8301−8309.
(43) Gribble, G. W. (2000) The natural production of organo-bromine compounds. *Environ. Sci. Pollut. Res. 7*, 37−47.
(44) Yadav, R. K., Dolai, S., Pal, S., and Adak, S. (2008) Role of tryptophan-208 residue in cytochrome c oxidation by ascorbate peroxidase from Leishmania major-kinetic studies on Trp208Phe mutant and wild type enzyme. *Biochim. Biophys. Acta, Proteins Proteomics 1784*, 863−871.
(45) Castro-Forero, A., Jiménez, D., López-Garriga, J., and Torres-Lugo, M. (2008) Immobilization of Myoglobin from Horse Skeletal Muscle in Hydrophilic Polymer Networks. *J. Appl. Polym. Sci. 107*, 881−890.
(46) Goral, V. N., and Ryabov, A. D. (1998) Reactivity of the horseradish peroxidase compounds I and II toward organometallic substrates. A stopped-flow kinetic study of oxidation of ferrocenes. *IUBMB Life 45*, 61−71.
(47) Chenprakhon, P., Sucharitakul, J., Panijpan, B., and Chaiyen, P. (2010) Measuring Binding Affinity of Protein-Ligand Interaction Using Spectrophotometry: Binding of Neutral Red to Riboflavin-Binding Protein. *J. Chem. Educ. 87*, 829−831.
(48) Otwinowski, Z., and Minor, W. (1997) Processing of X-ray diffraction data collected in oscillation mode. In *Methods in Enzymology* (Carter, C. W., Jr., and Sweet, R. M., Eds.) pp 307−326, Academic Press, New York.
(49) McCoy, A. J., Grosse-Kunstleve, R. W., Adams, P. D., Winn, M. D., Storoni, L. C., and Read, R. J. (2007) Phaser crystallographic software. *J. Appl. Crystallogr. 40*, 658−674.
(50) Adams, P. D., Afonine, P. V., Bunkoczi, G., Chen, V. B., Davis, I. W., Echols, N., Headd, J. J., Hung, L. W., Kapral, G. J., Grosse-Kunstleve, R. W., McCoy, A. J., Moriarty, N. W., Oeffner, R., Read, R. J., Richardson, D. C., Richardson, J. S., Terwilliger, T. C., and Zwart, P. H. (2010) PHENIX: a comprehensive Python-based system for macromolecular structure solution. *Acta Crystallogr., Sect. D: Biol. Crystallogr. 66*, 213−221.
(51) Collaborative Computational Project (1994) The CCP4 suite: programs for protein crystallography. *Acta Crystallogr., Sect. D: Biol. Crystallogr. 50*, 760−763.
(52) Emsley, P., Lohkamp, B., Scott, W. G., and Cowtan, K. (2010) Features and development of Coot. *Acta Crystallogr., Sect. D: Biol. Crystallogr. 66*, 486−501.
(53) Murshudov, G. N., Vagin, A. A., and Dodson, E. J. (1997) Refinement of Macromolecular Structures by the Maximum-Likelihood Method. *Acta Crystallogr., Sect. D: Biol. Crystallogr. 53*, 240−255.
(54) Afonine, P. V., Grosse-Kunstleve, R. W., Echols, N., Headd, J. J., Moriarty, N. W., Mustyakimov, M., Terwilliger, T. C., Urzhumtsev, A., Zwart, P. H., and Adams, P. D. (2012) Towards automated crystallographic structure refinement with phenix.refine. *Acta Crystallogr., Sect. D: Biol. Crystallogr. 68*, 352−367.
(55) Chen, Y. P., Woodin, S. A., Lincoln, D. E., and Lovell, C. R. (1996) An unusual dehalogenating peroxidase from the marine terebellid polychaete *Amphitrite ornata*. *J. Biol. Chem. 271*, 4609−4612.
(56) Thompson, M. K., Davis, M. F., de Serrano, V., Nicoletti, F. P., Howes, B. D., Smulevich, G., and Franzen, S. (2010) Internal binding of halogenated phenols in dehaloperoxidase-hemoglobin inhibits peroxidase function. *Biophys. J. 99*, 1586−1595.
(57) Tonami, H., Uyama, H., Nagahata, R., and Kobayashi, S. (2004) Guaiacol Oxidation Products in the Enzyme-Activity Assay Reaction by Horseradish Peroxidase Catalysis. *Chem. Lett. 33*, 796−797.
(58) Doerge, D. R., Divi, R. L., and Churchwell, M. I. (1997) Identification of the Colored Guaiacol Oxidation Product Produced by Peroxidases. *Anal. Biochem. 250*, 10−17.
(59) Simmons, K. E., Minard, R. D., and Bollag, J.-M. (1988) Oxidative Coupling and Polymerization of Guaiacol, a Lignin Derivative. *Soil Sci. Soc. Am. J. 52*, 1356−1360.
(60) de Serrano, V., and Franzen, S. (2012) Structural evidence for stabilization of inhibitor binding by a protein cavity in the dehaloperoxidase-hemoglobin from Amphitrite ornata. *Biopolymers 98*, 27−35.
(61) Sun, S., Sono, M., Du, J., and Dawson, J. H. (2014) Evidence of the direct involvement of the substrate TCP radical in functional switching from oxyferrous O_2 carrier to ferric peroxidase in the dual-function hemoglobin/dehaloperoxidase from *Amphitrite ornata*. *Biochemistry 53*, 4956−4969.
(62) Du, J., Sono, M., and Dawson, J. H. (2010) Functional switching of *Amphitrite ornata* dehaloperoxidase from O_2-binding globin to peroxidase enzyme facilitated by halophenol substrate and H_2O_2. *Biochemistry 49*, 6064−6069.
(63) Taurog, A., Dorris, M. L., and Guziec, F. S. (1992) An unexpected side reaction in the guaiacol assay for peroxidase. *Anal. Biochem. 205*, 271−277.
(64) Matsuo, T., Fukumoto, K., Watanabe, T., and Hayashi, T. (2011) Precise Design of Artificial Cofactors for Enhancing Peroxidase Activity of Myoglobin: Myoglobin Mutant H64D Reconstituted with a "Single-Winged Cofactor" Is Equivalent to Native Horseradish Peroxidase in Oxidation Activity. *Chem. - Asian J. 6*, 2491−2499.
(65) Sato, H., Hayashi, T., Ando, T., Hisaeda, Y., Ueno, T., and Watanabe, Y. (2004) Hybridization of Modified-Heme Reconstitution and Distal Histidine Mutation to Functionalize Sperm Whale Myoglobin. *J. Am. Chem. Soc. 126*, 436−437.
(66) Hayashi, T., Hitomi, Y., Ando, T., Mizutani, T., Hisaeda, Y., Kitagawa, S., and Ogoshi, H. (1999) Peroxidase Activity of Myoglobin Is Enhanced by Chemical Mutation of Heme-Propionates. *J. Am. Chem. Soc. 121*, 7747−7750.
(67) Banci, L., Ciofi-Baffoni, S., and Tien, M. (1999) Lignin and Mn Peroxidase-Catalyzed Oxidation of Phenolic Lignin Oligomers. *Biochemistry 38*, 3205−3210.
(68) Lindgren, B. O., Norman, N., Åselius, J., Refn, S., and Westin, G. (1960) Dehydrogenation of Phenols. II. Dehydrogenation Polymers from Guaiacol. *Acta Chem. Scand. 14*, 2089−2096.
(69) Schmalzl, K. J., Forsyth, C. M., and Evans, P. D. (1995) The reaction of guaiacol with iron III and chromium VI compounds as a model for wood surface modification. *Wood Sci. Technol. 29*, 307−319.

DOI: 10.1021/acs.biochem.8b00540
Biochemistry XXXX, XXX, XXX−XXX

(70) Lindgren, B. O., Norman, N., Åselius, J., Refn, S., and Westin, G. (1960) Dehydrogenation of Phenols. I. Dehydrogenation of 2,6-Dimethylphenol with Silver Oxide. *Acta Chem. Scand. 14*, 1203−1210.
(71) McKinley, A. B., Kenny, C. F., Martin, M. S., Ramos, E. A., Gannon, A. T., Johnson, T. V., and Dorman, S. C. (2004) Applications of absorption spectroelectrochemistry in artificial blood research. *Spectrosc. Lett. 37*, 275−287.
(72) Conant, J. B., and Pappenheimer, A. M., Jr. (1932) A redetermination of the oxidation potential of the hemoglobin-methemoglobin system. *J. Biol. Chem. 98*, 57−62.
(73) Heineman, W. R., Meckstroth, M. L., Norris, B. J., and Su, C.-H. (1979) Optically transparent thin layer electrode techniques for the study of biological redox systems. *J. Electroanal. Chem. Interfacial Electrochem. 104*, 577−585.
(74) Battistuzzi, G., Bellei, M., Casella, L., Bortolotti, C. A., Roncone, R., Monzani, E., and Sola, M. (2007) Redox reactivity of the heme Fe^{3+}/Fe^{2+} couple in native myoglobins and mutants with peroxidase-like activity. *JBIC, J. Biol. Inorg. Chem. 12*, 951−958.
(75) Battistuzzi, G., Bellei, M., Zederbauer, M., Furtmuller, P. G., Sola, M., and Obinger, C. (2006) Redox thermodynamics of the Fe(III)/Fe(II) couple of human myeloperoxidase in its high-spin and low-spin forms. *Biochemistry 45*, 12750−12755.
(76) Goodin, D. B., and McRee, D. E. (1993) The Asp-His-Fe triad of cytochrome *c* peroxidase controls the reduction potential, electronic structure, and coupling of the tryptophan free radical to the heme. *Biochemistry 32*, 3313−3324.
(77) Tanaka, M., Nagano, S., Ishimori, K., and Morishima, I. (1997) Hydrogen bond network in the distal site of peroxidases: spectroscopic properties of Asn70–> Asp horseradish peroxidase mutant. *Biochemistry 36*, 9791−9798.
(78) Osborne, R. L., Coggins, M. K., Raner, G. M., Walla, M., and Dawson, J. H. (2009) The mechanism of oxidative halophenol dehalogenation by *Amphitrite ornata* dehaloperoxidase is initiated by H_2O_2 binding and involves two consecutive one-electron steps: role of ferryl intermediates. *Biochemistry 48*, 4231−4238.
(79) Zhao, J., de Serrano, V., Zhao, J., Le, P., and Franzen, S. (2013) Structural and kinetic study of an internal substrate binding site in dehaloperoxidase-hemoglobin A from *Amphitrite ornata*. *Biochemistry 52*, 2427−2439.
(80) Dunford, H. B. (2016) Heme Peroxidase Kinetics. In *Heme Peroxidases*, Chapter 5, pp 99−112, The Royal Society of Chemistry.
(81) Franzen, S., Sasan, K., Sturgeon, B. E., Lyon, B. J., Battenburg, B. J., Gracz, H., Dumariah, R., and Ghiladi, R. (2012) Non-photochemical base-catalyzed hydroxylation of 2,6-dichloroquinone by H_2O_2 occurs by a radical mechanism. *J. Phys. Chem. B 116*, 1666−1676.
(82) Dunford, H. B., and Stillman, J. S. (1976) On the function and mechanism of action of peroxidases. *Coord. Chem. Rev. 19*, 187−251.

DOI: 10.1021/acs.biochem.8b00540
Biochemistry XXXX, XXX, XXX−XXX